analytical chemistry

pubs.acs.org/ac Article

J-Edited DIffusional Proton Nuclear Magnetic Resonance Spectroscopic Measurement of Glycoprotein and Supramolecular Phospholipid Biomarkers of Inflammation in Human Serum

Philipp Nitschke,* Samantha Lodge, Torben Kimhofer, Reika Masuda, Sze-How Bong, Drew Hall, Hartmut Schäfer, Manfred Spraul, Niels Pompe, Tammo Diercks, Ganeko Bernardo-Seisdedos, José M. Mato, Oscar Millet, Daniella Susic, Amanda Henry, Emad M El-Omar, Elaine Holmes, John C. Lindon, Jeremy K. Nicholson,* and Julien Wist*

Cite This: https://doi.org/10.1021/acs.analchem.1c04576 Read Online

ACCESS | Metrics & More | Article Recommendations | Supporting Information

ABSTRACT: Proton nuclear magnetic resonance (NMR) *N*-acetyl signals (Glyc) from glycoproteins and supramolecular phospholipids composite peak (SPC) from phospholipid quaternary nitrogen methyls in subcompartments of lipoprotein particles) can give important systemic metabolic information, but their absolute quantification is compromised by overlap with interfering resonances from lipoprotein lipids themselves. We present a J-Edited DIffusional (JEDI) proton NMR spectroscopic approach to selectively augment signals from the inflammatory marker peaks Glyc and SPCs in blood serum NMR spectra, which enables direct integration of peaks associated with molecules found in specific compartments. We explore a range of pulse sequences that allow editing based on peak J-modulation, translational diffusion, and T_2 relaxation time and validate them for untreated blood serum samples from SARS-CoV-2 infected patients (n = 116) as well as samples from healthy controls and pregnant women with physiological inflammation and hyperlipidemia (n = 631). The data show that JEDI is an improved approach to selectively investigate inflammatory signals in serum and may have widespread diagnostic applicability to disease states associated with systemic inflammation.

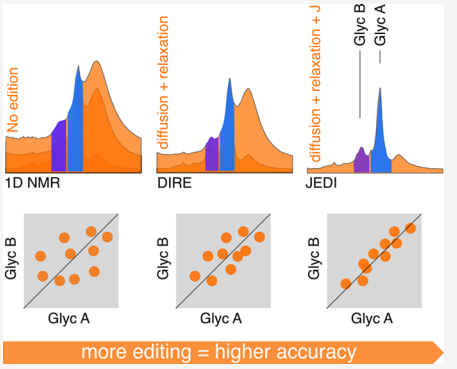

INTRODUCTION

Nuclear magnetic resonance (NMR) spectroscopy has been widely applied to multiple biomedical and physiological problems over the last three decades.[1] NMR spectroscopy is inherently quantitative and nondestructive with exceptionally high analytical reproducibility.[2,3] A key feature has been the ability to detect a wide range of chemical species of different molecular subclasses, sizes, and polarities at the same time and to go beyond concentration measurements into molecular compartmentation and dynamics giving extra dimensions of diagnostic potential. Apart from small-molecule studies that have multiple applications for many biofluids,[4,5] NMR is now the definitive tool for quantitative measurement of plasma lipoproteins and lipoprotein subfractions.[6−12]

Bell et al. first reported the application of proton NMR to detect α-1-acid-glycoprotein, an acute phase-reactive protein[13] in blood plasma associated with a number of inflammatory conditions. The proton NMR signals originating from the *N*-acetyls of *N*-acetylglucosamino and *N*-acetyl-galactosamino groups in the oligosaccharide side chains of glycoproteins have been measured in multiple studies on inflammatory processes including cardiovascular diseases,[14] rheumatoid arthritis,[15] and chronic obstructive pulmonary disease.[16] Inflammation is a normal physiological protective response to common infections and tissue injury that can become excessive and harmful on its own when unregulated, for example in the so-called cytokine storm.[17] Inflammation is also a mechanistically important part of most major diseases including cardiovascular disease, diabetes, cancers, and neurological conditions.[18] Although numerous inflammatory markers have been reported over the years including cytokines/chemokines,[19,20] lymphocytes,[21] C-reactive protein,[22] and prostaglandins,[23] there is an ongoing search for new inflammatory biomarkers and methodological approaches to quantify them quickly and more accurately.

Glyc is a ^{1}H NMR composite peak originating from the mobile −NAc methyl groups of glycan structures in glycosylated plasma proteins. It is currently subdivided into GlycA[24] (δ = 2.03; calibrated to glucose δ = 5.23) and GlycB

Received: October 22, 2021
Accepted: December 22, 2021

https://doi.org/10.1021/acs.analchem.1c04576
Anal. Chem. XXXX, XXX, XXX−XXX

(δ = 2.07; calibrated to glucose δ = 5.23) peaks.[25] The main signal contribution to Glyc is derived from five proteins, α-1-acid-glycoprotein, α1-antitrypsin, α1-antichymotrypsin, and haptoglobin where levels were shown to increase during inflammation while transferrin levels decreased.[24] Glyc has been shown to be a highly discriminatory factor for acute and chronic inflammation[14,26] in multiple medical conditions.[27−34] Our recent studies on elevated glycoprotein N-acetylation (GlycA and GlycB) in SARS-CoV-2 patients using diffusion and relaxation-edited (DIRE) spectroscopy also highlighted the role of a complex NMR signal, the intensity of which was strongly attenuated by the disease.[35] These supramolecular phospholipid composite (SPC) peaks,[35] subdivided in low- and high-frequency regions (SPC-A and SPC-B), were associated with the mobile choline headgroups ($-NMe_3^+$) of multiple phospholipids found in subcompartments of lipoprotein particles LDL and HDL, respectively.[9] We postulate that the signal intensity of SPCs is reduced significantly in systemic inflammation because of a reduced HDL particle number and composition,[35] in agreement with previous reports for HDL and LDL measurements using a range of clinical diagnostics methods.[36−39] This is consistent with lipidomic studies in individuals infected with the SARS-CoV-2 virus which showed reduced phospholipid levels[40−42] and the posterior normalization[27,43,44] and alterations observed in acute respiratory inflammatory conditions.[45]

Two types of experiments are widely used in high-throughput metabolic studies, standard water-suppressed ^{1}H-NMR, and T_2 relaxation-filtered (Carr−Purcell−Meiboom−Gill; CPMG) experiments.[46,47] The former contains contributions from high- and low-molecular-weight components, while the latter mostly retains contributions from small molecules (a lower molecular weight generally implies longer T_2 relaxation times). Consequently, complex modeling is required to extract lipoprotein parameters from spectra with a complex baseline and heavily overlapped peaks.[8,24,29,48,49] To simplify the observation of high-molecular-weight compounds, we have shown that the DIRE experiments yielded a subset of signals stemming from molecular partitions in high-molecular-weight structures with small diffusion coefficients[50] and retained a high degree of mobility resulting in sufficiently long T_2 times. Importantly, it enabled the direct observation of Glyc and SPCs.[35] One known disadvantage of the DIRE experiment is the coenhancement of other lipoprotein signals, resulting in the overlapping of Glyc with the allylic $-CH_2-$ lipoprotein ^{1}H resonances around δ = 1.95−2.10. Therefore, a new experimental approach is required for Glyc and SPCs for improved quantification accuracy. Spectroscopically, Glyc and SPCs share the common feature that they are singlets, that is, both the −NAc methyl groups (from Glyc) and the SPC-related $-^+NMe_3$ headgroups present isolated spin systems, whereas all overlapping resonances of interest (lipoproteins) are part of coupled spin systems. Scalar coupling can be used as a filtering mechanism, leaving SPCs and Glyc, while dephasing overlapping contributions from coupled spin systems.

In 2014, Martin-Pastor proposed the editing of singlet peaks based on a series of spin echoes for a range of coupling constants.[51] Combined with a z-filter, this sequence was shown to effectively dephase all coupled spin systems in the range of ∼3−16 Hz. However, the duration of this experiment (>400 ms for optimal editing) was impractical for detecting SPCs and Glyc, which have shorter T_2 relaxation times than low-molecular-weight metabolites. This experimental time cannot be shortened without reintroducing contributions from small molecules present in serum (or plasma) and would thus require an additional pulsed gradient scheme to remove residual antiphase contributions not suitable for high-throughput experiments. In summary, a compromise must be found between the effective removal of interfering signals by means of editing and retaining an acceptable signal-to-noise (S/N) ratio and baseline quality necessary for large cohort studies common in NMR-based metabolomics. Here, we propose the use of the J-Edited DIffusion (JEDI) NMR experiment, which combines relaxation and diffusion editing from DIRE with J-editing specifically customized to observe the inflammatory markers Glyc and SPC. This JEDI technique reduces overlap from lipoproteins, enables direct, simple integration of Glyc and SPCs in plasma or serum, and reveals additional spectral regions of Glyc.

EXPERIMENTAL METHODS

Participant Enrolment and Sample Collection. *Autonomous Community of the Basque Country (Spain).* The cohort consisted of (i) patients who tested positive for SARS-CoV-2 infection from upper and/or lower respiratory tract swabs by reverse transcription-polymerase chain reaction (RT-PCR) (n = 36) and (ii) healthy control participants (n = 80). All serum samples were collected by the Basque Biobank for research (BIOEF).[52,53] Healthy serum samples were collected before the COVID-19 pandemic from the active population while the COVID-19 samples were collected at the Cruces University Hospital (Barakaldo, Spain) from patients who presented compatible symptoms, confirmed by an RT-PCR assay on nasal swab samples. All participants provided informed consent to clinical investigations, according to the Declaration of Helsinki, and all data were anonymized to protect their confidentiality. The sample handling protocol was evaluated and approved by the *Comité de Ética de Investigación con medicamentos de Euskadi* (CEIm-E, PI+CES-BIOEF 2020-04 and PI219130). Shipment of human samples to ANPC had the approval of the Ministry of Health of the Spanish Government. Samples were stored at −80°C.

Microbiome Understanding in Maternity Studies. The cohort consisted of women (n = 99) who were recruited in their first trimester of pregnancy and followed through at seven time points: trimesters; one, two, and three, the time of birth and then 6 weeks, 6 months, and 12 months postpartum. All serum samples were collected at the University of New South Wales (UNSW), Microbiome Research Centre (MRC), Sydney, Australia. All participants provided informed consent to clinical investigations, according to the Declaration of Helsinki, and all data were anonymized to protect their confidentiality. The sample handling protocol was evaluated and approved by the South Eastern Sydney Local Health District Research Ethics Committee (17/293 (HREC/17/POWH/605)). Shipment of human samples to ANPC had the approval of the University of New South Wales. Samples were stored at −80°C.

Sample Preparation and Data Acquisition. *^{1}H NMR Sample Preparation.* Serum samples were thawed at 20 °C for 30 min and then centrifuged for 10 min at 13,000 g at 4 °C. All samples were prepared in 5 mm outer-diameter SampleJet NMR tubes, following the recommended procedures for in vitro analytical and diagnostics procedures[54] using 300 μL of serum mixed with 300 μL phosphate buffer (75 mM Na_2HPO_4, 2 mM NaN_3, 4.6 mM sodium trimethylsilyl

https://doi.org/10.1021/acs.analchem.1c04576
Anal. Chem. XXXX, XXX, XXX−XXX

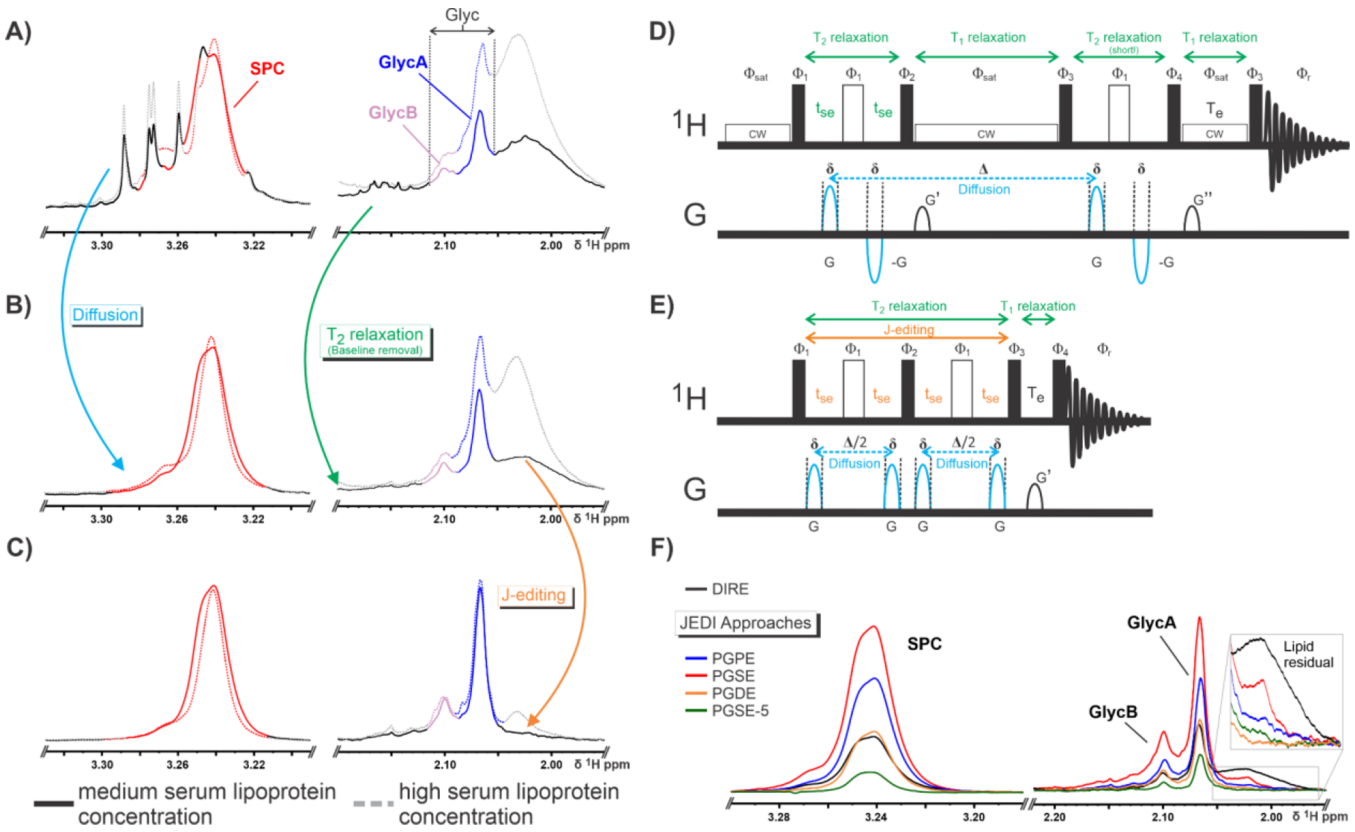

Figure 1. JEDI approach combines the NMR spectroscopic methodologies of J-editing, diffusion, and relaxation to selectively highlight the biomarkers SPC and Glyc (GlycA+B) in human serum and plasma. (A–C) Proton spectra focusing on the SPC (red) and Glyc (GlycA+B; blue +pink) regions with (A) 1D ^{1}H with solvent suppression showing full convolution of SPC and Glyc by small molecules, protein background, and lipoproteins; (B) DIRE spectrum removing overlap from small molecules (diffusion) and protein background (T_2 relaxation) but leaving lipoprotein signatures largely intact; (C) JEDI-PGPE additionally removing overlap from lipoprotein resonances allowing for straightforward integration of SPC and Glyc; (D) DIRE pulse sequence according to Lodge et al.[35] highlighting its editing methodologies of relaxation and diffusion; (E) JEDI-PGPE pulse sequence highlighting the different spectroscopic editing methodologies of diffusion, relaxation, and J-editing (for a detailed explanation of the parameters see Supporting Information section Basic Pulse Sequence and Idea of JEDI); (F) S/N comparison of various JEDI approaches to the established DIRE method for SPC and Glyc (GlycA+B).

propionate-[2,2,3,3-$^2H_4$] (TSP) in H_2O/D_2O 4:1, pH 7.4 ± 0.1, purchased from Bruker A.G. Rheinstetten). Additionally, the samples were sonicated for 5 min at ambient temperature prior to analysis. Plasma samples were from the ANPC long-term reference stock and were prepared using the same method as that for serum.

^{1}H NMR Spectroscopy Data Acquisition and Processing Parameters. NMR spectroscopic analyses were performed on two 600 MHz Bruker Avance III HD spectrometers, each equipped with a 5 mm BBI probe and fitted with a Bruker SampleJet robot cooling system set to 5 °C. A full quantitative calibration was completed prior to the analysis using a protocol described elsewhere.[54]

The standard one-dimensional (1D) experiments with solvent suppression (pp: noesygppr1d) were acquired with 32 scans (+4 dummy scans), 98k data points, relaxation delay of 4.0 s, and a spectral width of 30 ppm resulting in a total experimental time of 4 min 3 s (according to the Bruker In Vitro Diagnostics research IVDr methods). The CPMG experiments with solvent suppression (pp: cpmgpr1d) were performed with 32 scans (+4 dummy scans), 74k data points, relaxation delay of 4.0 s, and a spectral width of 20 ppm resulting in a total experimental time of 3 min 58 s (according to the Bruker In Vitro Diagnostics research IVDr methods).

DIRE and the JEDI sequences (PGPE, PGSE, PGPDE, and PGSE-5) were acquired with 64 scans, 98k data points, relaxation delay of 1.0 s, and a spectral width of 30 ppm resulting in a total experimental time of 4 min 25 s for DIRE, 4 min 23 s for JEDI-PGPE, 4 min 20 s for JEDI-PGSE, 4 min 27 s for JEDI-PGDE, and 4 min 26 s for JEDI-PGSE-5. Further experimental parameters for DIRE and the other JEDI sequences (PGPE, PGSE, PGDE, and PGSE-5) are presented in Figures 1 and Supporting Information S6–S10.

The (semi)selective total correlation spectroscopy (TOCSY) experiments (pp: *selmlgp* + added presaturation for water suppression) were acquired with 64 scans, 64k data points, a relaxation delay of 2.0 s, and a spectral width of 20 ppm. TOCSY mixing time was set to 40 ms, and selective excitation of the allylic lipid sp2 double bond region was achieved by refocusing the resonances around δ = 5.3 with a 10 ms 180° Gaussian pulse. The (semi)selective TOCSY experiments also excite the anomeric glucose peak at δ = 5.23, but the resulting TOCSY peaks (δ = 3.71, 3.53, and 3.41) do not interfere with the desired lipid resonances from δ = ~1.9–2.1 (data not shown).

For the spike-in experiments, a plasma sample was thawed and acquired as stated above. The sample was then removed from the magnet, and 2 μL of a lipid mix (Taken from the lipid emulsion of an OLIMEL N9-840E emulsion for intravenous

https://doi.org/10.1021/acs.analchem.1c04576
Anal. Chem. XXXX, XXX, XXX–XXX

infusion; 200 mL containing 200 g refined olive oil and refined soya oil (~4:1), 22.5 g glycerol, 12.5 g egg lecithin, 0.3 g sodium oleate, sodium hydroxide (for pH adjustment), and water) was added directly into the plasma. The sample was shaken thoroughly and sonicated for 15 min to allow for incorporation of the lipid mix into the lipoprotein particles. Subsequent measurements (IVDr, JEDI, DIRE, etc.) were carried out as stated above.

Time-domain data were Fourier transformed and processed in automation using Bruker Topspin 3.6.2 or Bruker Topspin 4.0.9 and ICON NMR to obtain phase- and baseline-corrected spectra. An exponential line broadening of 0.3 Hz was applied to the 1D water-suppressed and CPMG experiments, whereas a broadening of 1 Hz was applied to the DIRE and JEDI free induction decays (FIDs). For the JEDI sequences, only the first 32 K real data points were Fourier transformed to reduce unwanted noise contributions from the FID.

All DIRE and JEDI spectra were calibrated by setting the spectral reference value to 0 (SR = 0), that is, "no calibration." The *N*-acetyl residues of Glyc and the $-NMe_3^+$ moieties of SPCs show constant chemical shift behavior and are not perturbed by intersample variation found in serum or plasma (see also Figure S2). Usually, serum and/or plasma are calibrated to the methyl group of alanine at δ = 1.47 or the anomeric proton of glucose at δ = 5.23. DIRE and JEDI remove the contributions from small molecules including alanine and glucose by diffusion. Hence, calibration to alanine or glucose is not possible, and alternative calibration procedures were not followed up upon in detail as the SR = 0 yielded superb alignment results for DIRE and JEDI. In addition, aligning the spectra to Glyc or SPCs itself is not straightforward for large datasets. Because of the heterogeneous nature of Glyc (at least six glycoproteins: α-1-acid-glycoprotein, α1-antitrypsin, α1-antichymotrypsin, haptoglobin, transferrin, and fibrinogen) the maximum of the composite can slightly change depending on the relative concentration of the subcomponents. The SPC presents a similar problem stemming from HDL and LDL particles, that is, different concentrations of the subcomponents lead to a shifting maximum. As a result of calibration using SR = 0, the chemical shift of GlycA+B and SPCs is slightly different compared to previous literature reports.[35] In this work, GlycA resonates at δ = 2.07 (instead of δ = 2.03) and GlycB at δ = 2.10 (instead of δ = 2.07), and the SPC region is defined as δ = 3.17−3.33 (instead of δ = 3.20−3.30).

The ERETIC[55] correction was applied to all spectra to ensure that the observed intensities are quantitative. The ERETIC factor is automatically generated from the ERETIC signal and saved in an XML file called "QuantFactorSample" for each sample.

NMR Data Analysis. The integration of the GlycA, GlycB, and SPC peaks and the subsequent statistical analysis were performed using scripts for the R Statistical Software using standard functions. Integration of the peaks is achieved readily by summation of a fixed spectra region (GlycA: δ = 2.05−2.09; GlycB: δ = 2.09−2.12; SPC: δ = 3.15−3.35). Hence, optimal calibration of the spectra is critical. Following the IVDr procedure, all spectra are aligned to the TSP peak measured in the water-suppressed 1D experiment. Better results (see Figure S2) have been obtained, however, without calibration to TSP.

RESULTS AND DISCUSSION

We demonstrate the JEDI NMR approach to recover metabolic inflammatory biomarker information using a mixed sample set from (1) patients infected with SARS-CoV-2 and their controls and (2) pregnant women. The first dataset provides a wide range of inflammatory levels and associated variation in SPC and Glyc levels,[27,56] while the second dataset provides serum profiles with increased lipoprotein levels and mild inflammation.[57,58]

JEDI Provides Inflammation Marker Quantification by Simple Peak Integration. In a regular ^{1}H NMR spectrum of serum (Figure 1A) with medium (black trace) and high (gray trace) concentration of lipoproteins, SPC (red) and Glyc (blue and pink; 2.07 and 2.1 ppm (see the section Sample Preparation and Data Acquisition) are highly intricate showing interfering resonances from small molecules, lipoproteins, and an overall protein background (Figures 1A, S1A and S1G). The introduction of T_2 relaxation to filter out the broad protein envelope by applying a CPMG pulse train yields a flat baseline as a first editing step (Figure S1B and S1H). DIRE[50] adds another layer of editing by combining T_2 relaxation and diffusion to create a spectrum devoid of small-molecule contributions and direct protein background (Figures 1B, S1C and S1I). The DIRE experiment already allows for integration of SPC (red) but Glyc (especially GlycA) is overlapped with the allylic $-CH_2-$ stemming from lipoproteins, which are not significantly attenuated by the double filtering. However, the lipoprotein interference can be effectively attenuated by incorporating J-modulation in addition to T_2 relaxation and diffusion resulting in a triple edition experiment summarized as JEDI NMR. The J-modulation results in interference attenuation of the signal. Figure 1C shows how the application of JEDI yields a clean spectrum that allows clear observation of the two biomarkers of interest. For JEDI, $-^+NMe_3$ of SPCs and the *N*-acetyls of Glyc are refocused because of the absence of homonuclear J coupling in these isolated spin systems, which allow selective integrals. By contrast, other J coupled systems get largely defocused enabling integration with less interference from lipids. With JEDI, SPCs and Glyc can simply be integrated bypassing potential ambiguity from so far employed signal fitting methods.[8,14,24,29,48,49]

Evaluation of the Effectiveness of JEDI to Filter Lipoprotein Contributions in Various Inflammatory States. Focusing on a serum sample with high levels of lipid/lipoprotein (gray trace) in Figure 1C, it is apparent that a residual lipoprotein signal is surviving the intensive spectral editing of JEDI. To investigate the influence of these residual lipoproteins, JEDI spectra of 63 serum samples from a cohort of 99 pregnant women were overlapped (see the subsection "Participant Enrolment and Sample Collection" of the Supporting Information and Figure S2). Although the overlapped sera show a high variance in the residual lipoprotein signal, the GlycA pattern is not affected at all. This suggests that there is no significant residual signal "hidden" below Glyc, which correlates with the residual lipoprotein signal. To further test the robustness of the JEDI, an artificial outlier was created by spiking a lipid mixture from a complex parenteral nutrition fluid into a serum sample (Figure S3). The regular proton spectrum and DIRE (Figure S3A and B) are heavily influenced by the addition of the lipid mixture, almost doubling the "observed" GlycA integral for the

https://doi.org/10.1021/acs.analchem.1c04576
Anal. Chem. XXXX, XXX, XXX−XXX

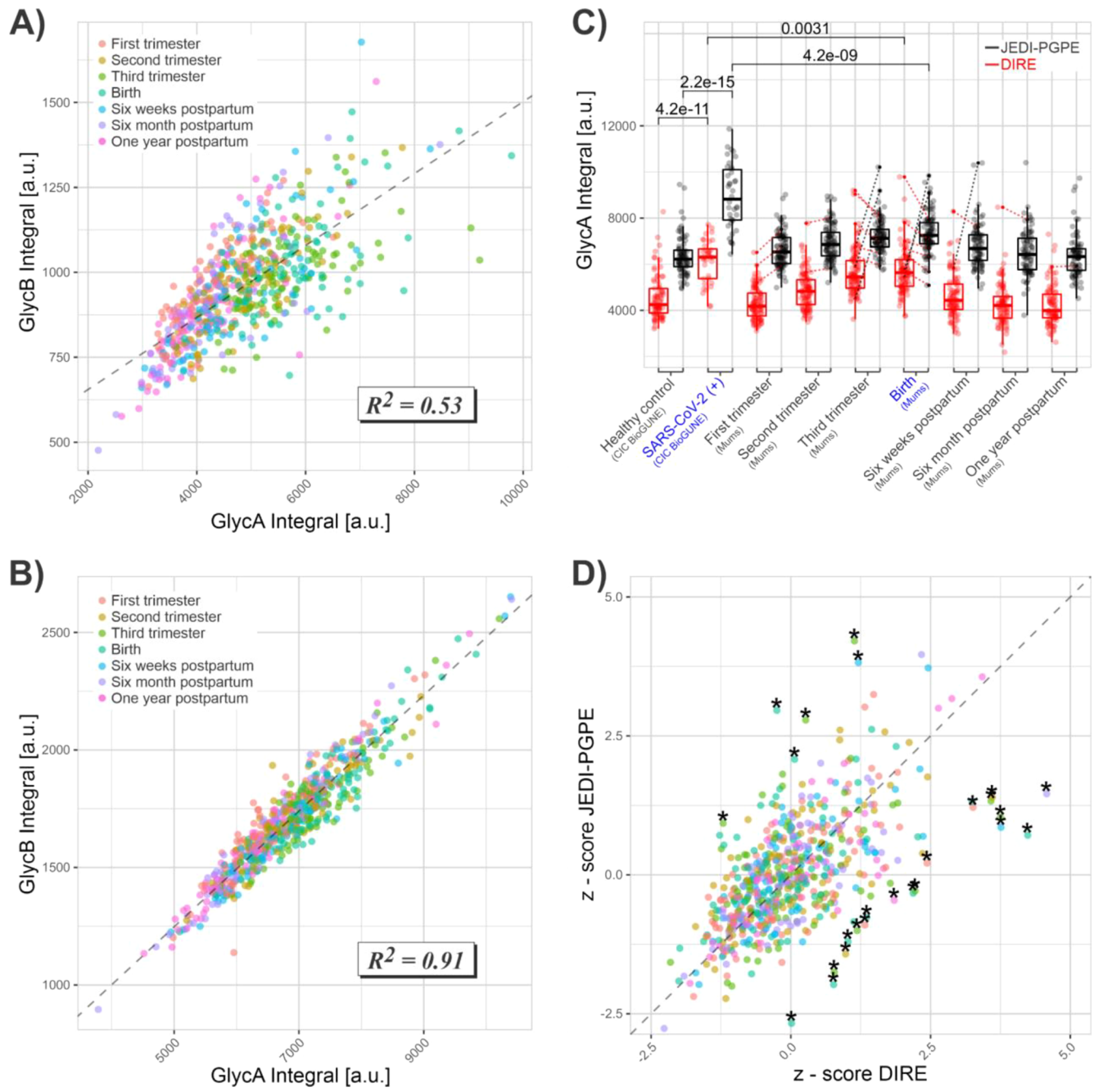

Figure 2. Statistical analyses comparing JEDI and DIRE for a dataset of 631 longitudinally collected serum samples of pregnant women (University of New South Wales, Australia) and a dataset from CIC BioGUNE (Spain) containing 116 samples of healthy (n = 80) and SARS-CoV-2(+) (n = 36) specimens. (A) Linear fit for the relationship of GlyA and GlycB by the DIRE experiment. Only a weak correlation can be found because of the DIRE data being scrambled by the overlapping lipoprotein peaks. (B) Linear fit for the relationship of GlyA and GlycB by the JEDI-PGPE experiment. In contrast to DIRE, the JEDI-PGPE reveals a high correlation between GlycA and B indicating that despite their heterogeneous nature the ratio of underlying glycoproteins remains fairly constant. (C) Box plots showing the GlycA integral for the longitudinal serum samples of pregnant women and CIC BioGUNE samples measured by DIRE (red) and JEDI-PGPE (black). Both techniques readily distinguish healthy and SARS-CoV-2 positive samples. (D) Z-scores indicating which samples changed their respective rank ("mis-classification") for DIRE against JEDI. Strongest outliers are marked with an asterisk.

DIRE spectrum. In contrast, for JEDI the GlycA integral is largely unaffected (<5%) yielding a reliable integration result even for a spectrum with an artificial lipid signal higher in intensity than ever witnessed in our institute (>10,000 samples to date) (Figure S3C). In another control experiment, the lipoprotein signal itself was investigated by selective TOCSY (Figure S4). Here, the comparison of DIRE, JEDI, and selective TOCSY spectra showed that the JEDI and the selective TOCSY can reproduce the DIRE pattern further indicating the absence of hidden interference signals below Glyc in the JEDI. Additionally, the selective TOCSY spectra show a high degree of heterogeneity of the lipoprotein response between different serum samples (Figure S4A–C). In fact, even similar DIRE spectra according to visual inspection (Figure S4A vs B) can have a quite different lipoprotein envelope. This is represented in a high-frequency "shoulder"

https://doi.org/10.1021/acs.analchem.1c04576
Anal. Chem. XXXX, XXX, XXX−XXX

that perfectly overlaps with GlycA, which further skews results extracted using DIRE or fitting methods but is circumvented using JEDI. Interestingly, comparing the lipoprotein signature obtained from the selective TOCSY spectra with the ones obtained from spiked lipid mixture spectra suggests that the high-frequency shoulder of the lipoproteins is more attenuated than its low-frequency counterpart (Figure S5), which further enforces the robustness of the JEDI technique. This improved suppression is possible because of a different coupling constant of the underlying resonances in the shoulder for the J-editing or because of different relaxation properties of the high- and low-frequency partitions (see Supporting Information section Effectiveness of the J-editing for Different Lipoprotein Moieties).

Optimal Parameters for the JEDI-PGPE Are Chosen To Find a Compromise between the Acceptable *S/N* Ratio and Effective Removal of the Interfering Peaks. Figure 1D depicts the current DIRE sequence, which is based on a stimulated echo (STE) experiment with an eddy current delay (bruker pp.: *ledbpgppr2s1d*), whereas the delays in the first spin echo (t_{se}) are significantly increased (16.6 ms) to allow for additional T_2 relaxation. Otherwise, the predominant relaxation pathway for the DIRE is T_1 relaxation. To defocus signals by J-editing, long evolution times in the *xy*-plane (dominated by T_2 relaxation, optimally 1/(2 J) for the full spin echo; for the respective coupling) are required. Hence, the STE sequence is not ideal to incorporate J-editing as it would only lead to a needlessly long sequence with long T_1 and T_2 relaxation segments. In contrast, a less sophisticated sequence employing mainly T_2 relaxation like the oldest diffusion experiment pulsed gradient spin echo (PGSE), which goes in line with the suggested ^{1}H s-filtered sequence,[51] is a more promising approach. Figure 1E shows our employed JEDI sequence, the pulsed gradient perfect echo (PGPE), and highlights the main editing approaches of relaxation (green), diffusion (light blue), and J-editing (orange). In addition, JEDI-PGPE does not require any additional solvent suppression scheme when applied to serum and plasma samples. An in-depth discussion of the sequence and its parameters can be found in the Supporting Information (section Basic Pulse Sequences and Idea of JEDI).

Next to the JEDI-PGPE, three other related JEDI sequences were tested: The PGSE, the pulsed gradient double echo (PGDE), and the Pulsed Gradient Spin Echo × 5 (PGSE-5). All sequences are based on one or multiple concatenated spin echoes employing varying refocusing delays (see Figures S8−S10). A direct comparison of the new JEDI sequences (PGPE, blue; PGSE, red; PGDE, orange; PGSE-5, green) to the DIRE (black) sequence for the two biomarkers SPC and Glyc is depicted in Figure 1F. The experimental parameters were adjusted so every experiment would have an approximate duration of 4.5 min as time is crucial in clinical laboratories. It is evident that JEDI sequences are capable of defocusing the overlapping lipoprotein resonances but show significant differences in the resulting signal intensity (Table S1 and Figures S11 and S12). Here, the JEDI-PGSE and the JEDI-PGPE have by far the highest *S/N* ratio (SPC: 820.4 and GlycA: 382.9 for JEDI-PGSE and SPC: 578.0 and GlycA: 256.1 for JEDI-PGPE; Sample 1 in Table S1) with effective suppression of interfering peaks. While its simplicity and high *S/N* ratio make JEDI-PGSE an ideal candidate, it leads to residual antiphase contributions, which are not acceptable (Figure S13). Both the JEDI-PGDE and JEDI-PGSE-5 perform well, but for a low *S/N* ratio (SPC: 293.9 and GlycA: 154.3 for JEDI-PGDE and SPC: 97.3 and GlycA: 78.5 for JEDI-PGSE-5; Sample 1 in Table S1); especially for SPC-B. In summary, the JEDI-PGPE yielded the best performance for applied criteria of high-throughput NMR metabolomics, greatly outperforming the DIRE on Glyc determination and doubling the *S/N* ratio.

JEDI Spectra of Serum and Plasma Differ Only by the Contributions of Fibrinogen. As expected, the spectra look identical apart from a minor peak (δ = 2.13) in the high-frequency region of Glyc, which is present in plasma but absent in serum (Figure S14A). A major difference between serum and plasma is the absence of clotting factors with fibrinogen as its main contributor. Therefore, a spike-in experiment with fibrinogen was performed, indeed identifying fibrinogen as an additional contributor to Glyc (Figure S14B) showing that the JEDI-PGPE gives new insights into the underlying nature of Glyc and reveals that Glyc has additional resonances at the higher frequency to the previously described regions of GlycA and GlycB.

JEDI Approach Validated in Two-Patient Cohorts. We investigated the performance of the JEDI-PGPE against DIRE using longitudinally sampled sera from 99 pregnant women, following them during pregnancy, at birth, and up to 1 year postpartum (trimester 1, 2, and 3, birth, 6 weeks postpartum, 6 months postpartum, and 1 year postpartum = 7 time points) resulting in 631 serum samples. This cohort provides samples with increased lipoprotein concentrations[57,58] that are expected to modulate GlycA and GlycB peaks differently for DIRE. Because both stem from the same structures, their integral is expected to be highly correlated in the JEDI-PGPE. In contrast, it is expected that both DIRE and JEDI-PGPE yield similar results for SPCs. Integrals of GlycA+B and SPC were extracted from both DIRE and JEDI-PGPE spectra for the cohort of pregnant women as well as for the Spanish COVID-19 cohort.

Comparison of GlycA vs GlycB concentrations obtained using DIRE and JEDI (Figure 2A,B) reveals significantly higher correlation (R^2 of 0.91) for the latter than the former (R^2 of 0.53). Lipoprotein concentrations are increased during pregnancy; hence, it is expected that DIRE reports an "artificial" increase in GlycA over the course of pregnancy because of its partial overlap with the allylic $-CH_2-$ of the lipoproteins. Indeed, DIRE shows a sustained increase for the GlycA integral during the three trimesters peaking at birth and a steep return to lower levels postpartum. The JEDI-PGPE shows a similar trend, but both the increase and decrease are less pronounced. The differences between DIRE and JEDI-PGPE spectra become evident when the GlycA trajectory during pregnancy is compared to the COVID infected people from the CIC Biogune cohort. Although both DIRE and JEDI-PGPE are effectively discriminating between healthy and SARS-CoV-2 infected (acute phase) individuals, DIRE data suggest that the GlycA level in late-stage pregnancy is comparable to that in an acute inflammatory disease like SARS-Cov-2 (Figure 2C, blue titles, p = 0.0031). In contrast, JEDI-PGPE perfectly discriminates ($p = 4.2 \times 10^{-9}$) between samples taken from people in late-stage pregnancy (a physiologically inflammatory state) and those with acute SARS-CoV-2(+) infection yielding by far the highest GlycA values. Additionally, Figure 2C demonstrates the two fold increase in the *S/N* ratio achieved by JEDI-PGPE.

https://doi.org/10.1021/acs.analchem.1c04576
Anal. Chem. XXXX, XXX, XXX−XXX

Moreover, as the error in GlycA induced by lipoprotein contribution varies between samples, removing it will alter their respective rank in the distribution of concentration, as illustrated in Figure 2D. The z-scores obtained using DIRE are compared with the ones measured by JEDI. Samples along the diagonal conserve their rank (same z-score for both experiments), while samples away from the diagonal are reclassified, yet the z-scores plot shows a high level of dispersion indicating that many samples are assigned to different ranks. Outliers are marked with an asterisk if $\text{z-score}_{\text{DIRE}} - \text{z-score}_{\text{JEDI}} > 2$ (below diagonal) or if $\text{z-score}_{\text{DIRE}} - \text{z-score}_{\text{JEDI}} < -2$ (above diagonal). These outliers are also highlighted in Figure 2C by dotted red and black lines, respectively. A similar comparison of the SPC integral for DIRE and the JEDI-PGPE shows a higher correlation (R^2 = 0.89) between both sequences (Figure S15). This is expected as the DIRE already removes interfering signals from SPCs and minor deviations between DIRE and JEDI-PGPE are rooted in the different relaxation pathways leading to a different SPC-A/SPC-B ratio (see Supporting Information section SPC for DIRE and JEDI-PGPE and Figure S16). Overall, these analyses demonstrate the clear superiority of the JEDI-PGPE over DIRE for the quantification of the GlycA and GlycB biomarkers, yielding increased *S*/*N* ratios. There is currently much interest in the use of NMR technologies to understand inflammatory conditions and diseases including COVID-19 and the systemic recovery trajectories from COVID-19 including monitoring of phenoreversion in postacute COVID-19 syndrome.[27,56,59,60] The JEDI NMR experiment has now been demonstrated to be a useful tool in that process as it can accurately quantify important immune-metabolic markers of the disease.

CONCLUSIONS

The JEDI NMR method combines three independent spectroscopic editing techniques (relaxation, diffusion, and J-editing) in a single compact experiment. JEDI allows the precise and direct determination of the inflammatory biomarkers SPC, GlycA, and GlycB by simple integration. JEDI eliminates other convoluting resonances stemming from large proteins, small molecules, and lipoprotein particles while retaining a high *S*/*N* ratio, thereby making JEDI suitable for high-throughput diagnostic NMR studies. Furthermore, JEDI was shown to be superior to the DIRE approach by revealing the high correlation between the Glyc compartments GlycA and GlycB and an increased discriminating power between different medical conditions, that is, inflammatory disease (here COVID-19) as well as late-stage pregnancy. In addition to the main JEDI-PGPE experiment, a series of other JEDI pulse sequences are described offering a higher *S*/*N* ratio or improved lipoprotein suppression for application to other problems at hand. Overall, JEDI as a tool in the NMR metabolic toolbox provides a high-fidelity determination of the biomarkers SPC and Glyc which will be useful in assessing severity and recovery from Post-Acute COVID-19 Syndrome (PACS) and other inflammatory conditions and will open the pathway to a more detailed description of these heterogeneous biomarkers in the future.

ASSOCIATED CONTENT

Supporting Information

The Supporting Information is available free of charge at https://pubs.acs.org/doi/10.1021/acs.analchem.1c04576.

Comparison of 1D ^{1}H, CPMG, DIRE, and JEDI spectra, Glyc region for 63 serum samples, Glyc region for a plasma sample spiked with parenteral nutrition fluid, decomposition of Glyc peak contributions, effectiveness of JEDI, DIRE pulse sequence, and JEDI pulse sequences, comparison of *S*/*N* for different pulse sequences, DIRE vs JEDI for serum with medium concentration of lipoproteins, DIRE vs JEDI for serum with a high concentration of lipoproteins, antiphase residuals in the PGSE spectrum, detection of fibrinogen, and DIRE vs JEDI correlation for SPC peak integral (PDF)

AUTHOR INFORMATION

Corresponding Authors

Philipp Nitschke − *Australian National Phenome Centre and Computational and Systems Medicine, Health Futures Institute, Murdoch University, Perth, Western Australia 6150, Australia*; Email: Philipp.Nitschke@murdoch.edu.au

Jeremy K. Nicholson − *Australian National Phenome Centre and Computational and Systems Medicine, Health Futures Institute, Murdoch University, Perth, Western Australia 6150, Australia; Institute of Global Health Innovation Faculty of Medicine, Imperial College London, London SW7 2NA, U.K.*; orcid.org/0000-0002-8123-8349; Email: Jeremy.Nicholson@murdoch.edu.au

Julien Wist − *Australian National Phenome Centre and Computational and Systems Medicine, Health Futures Institute, Murdoch University, Perth, Western Australia 6150, Australia; Chemistry Department, Universidad del Valle, Cali 76001, Colombia*; orcid.org/0000-0002-3416-2572; Email: Julien.Wist@murdoch.edu.au, julien.wist@correounivalle.edu.co

Authors

Samantha Lodge − *Australian National Phenome Centre and Computational and Systems Medicine, Health Futures Institute, Murdoch University, Perth, Western Australia 6150, Australia*; orcid.org/0000-0001-9193-0462

Torben Kimhofer − *Australian National Phenome Centre and Computational and Systems Medicine, Health Futures Institute, Murdoch University, Perth, Western Australia 6150, Australia*; orcid.org/0000-0001-7158-9930

Reika Masuda − *Australian National Phenome Centre and Computational and Systems Medicine, Health Futures Institute, Murdoch University, Perth, Western Australia 6150, Australia*

Sze-How Bong − *Australian National Phenome Centre and Computational and Systems Medicine, Health Futures Institute, Murdoch University, Perth, Western Australia 6150, Australia*; orcid.org/0000-0002-3313-5097

Drew Hall − *Australian National Phenome Centre and Computational and Systems Medicine, Health Futures Institute, Murdoch University, Perth, Western Australia 6150, Australia*

Hartmut Schäfer − *Bruker Biospin GmbH, Rheinstetten 76287, Germany*

Manfred Spraul − *Bruker Biospin GmbH, Rheinstetten 76287, Germany*

Niels Pompe − *Bruker Biospin GmbH, Rheinstetten 76287, Germany*

https://doi.org/10.1021/acs.analchem.1c04576
Anal. Chem. XXXX, XXX, XXX−XXX

Tammo Diercks − *Precision Medicine and Metabolism Laboratory, CIC bioGUNE, Parque Tecnológico de Bizkaia, Derio 48160, Spain*
Ganeko Bernardo-Seisdedos − *Precision Medicine and Metabolism Laboratory, CIC bioGUNE, Parque Tecnológico de Bizkaia, Derio 48160, Spain*
José M. Mato − *Precision Medicine and Metabolism Laboratory, CIC bioGUNE, Parque Tecnológico de Bizkaia, Derio 48160, Spain*
Oscar Millet − *Precision Medicine and Metabolism Laboratory, CIC bioGUNE, Parque Tecnológico de Bizkaia, Derio 48160, Spain;* orcid.org/0000-0001-8748-4105
Daniella Susic − *School of Women's and Children's Health, University of New South Wales, Sydney, New South Wales 2052, Australia; UNSW Microbiome Research Centre, St George Hospital, Kogarah, New South Wales 2217, Australia*
Amanda Henry − *School of Women's and Children's Health, University of New South Wales, Sydney, New South Wales 2052, Australia; UNSW Microbiome Research Centre, St George Hospital, Kogarah, New South Wales 2217, Australia*
Emad M El-Omar − *Microbiome Research Centre, St George & Sutherland Clinical School, University of New South Wales, Sydney, New South Wales 2052, Australia*
Elaine Holmes − *Australian National Phenome Centre and Computational and Systems Medicine, Health Futures Institute, Murdoch University, Perth, Western Australia 6150, Australia; Department of Metabolism, Digestion and Reproduction, Faculty of Medicine, Imperial College London, London SW7 2AZ, U.K.*
John C. Lindon − *Department of Metabolism, Digestion and Reproduction, Faculty of Medicine, Imperial College London, London SW7 2AZ, U.K.;* orcid.org/0000-0002-0916-6360

Complete contact information is available at: https://pubs.acs.org/10.1021/acs.analchem.1c04576

Notes

The authors declare no competing financial interest.

■ ACKNOWLEDGMENTS

We thank The Spinnaker Health Research Foundation, WA, The McCusker Charitable Foundation, WA, The Western Australian State Government, and the Commonwealth Department of Health for funding the Australian National Phenome Centre for this and related work via its Medical Research Future Fund (MRFF) Accelerated Research. We thank the Department of Jobs, Tourism, Science and Innovation and its Premier's Science Fellowship Program for funding RLL and EH; and the Australian Research Council (ARC) for its Australian Laureate Fellowship (FL200100220) funding for EH. We also would like to acknowledge the Covid Research Response Team (CRR), for the coordination, sampling, and biobanking of patient samples and clinical metadata. We thank Prof. Bu B. Yeap for providing us with parenteral nutrition fluid.

■ REFERENCES

(1) Nicholson, J. K.; Holmes, E.; Kinross, J. M.; Darzi, A. W.; Takats, Z.; Lindon, J. C. *Nature* **2012**, *491*, 384−392.
(2) Dumas, M.-E.; Maibaum, E. C.; Teague, C.; Ueshima, H.; Zhou, B.; Lindon, J. C.; Nicholson, J. K.; Stamler, J.; Elliott, P.; Chan, Q.; Holmes, E. *Anal. Chem.* **2006**, *78*, 2199−2208.
(3) Keun, H. C.; Ebbels, T. M. D.; Antti, H.; Bollard, M. E.; Beckonert, O.; Schlotterbeck, G.; Senn, H.; Niederhauser, U.; Holmes, E.; Lindon, J. C.; Nicholson, J. K. *Chem. Res. Toxicol.* **2002**, *15*, 1380−1386.
(4) Nicholson, J. K.; Wilson, I. D. *Prog. Nucl. Magn. Reson. Spectrosc.* **1989**, *21*, 449−501.
(5) Rabenstein, D. L. *J. Biochem. Biophys. Methods* **1984**, *9*, 277−306.
(6) Ala-Korpela, M.; Korhonen, A.; Keisala, J.; Hörkkö, S.; Korpi, P.; Ingman, L. P.; Jokisaari, J.; Savolainen, M. J.; Kesäniemi, Y. A. *J. Lipid Res.* **1994**, *35*, 2292−2304.
(7) Khakimov, B.; Hoefsloot, H. C. J.; Mobaraki, N.; Aru, V.; Kristensen, M.; Lind, M. V.; Holm, L.; Castro-Mejía, J. L.; Nielsen, D. S.; Jacobs, D. M.; Smilde, A. K.; Engelsen, S. B. *bioRxiv* **2021**, No. 432509.
(8) Otvos, J. D.; Jeyarajah, E. J.; Bennett, D. W. *Clin. Chem.* **1991**, *37*, 377−386.
(9) Baumstark, D.; Kremer, W.; Boettcher, A.; Schreier, C.; Sander, P.; Schmitz, G.; Kirchhoefer, R.; Huber, F.; Kalbitzer, H. R. *J. Lipid Res.* **2019**, *60*, 1516−1534.
(10) Monsonis Centelles, S.; Hoefsloot, H. C. J.; Khakimov, B.; Ebrahimi, P.; Lind, M. V.; Kristensen, M.; de Roo, N.; Jacobs, D. M.; van Duynhoven, J.; Cannet, C.; Fang, F.; Humpfer, E.; Schäfer, H.; Spraul, M.; Engelsen, S. B.; Smilde, A. K. *Anal. Chem.* **2017**, *89*, 8004−8012.
(11) Jimenez, B.; Holmes, E.; Heude, C.; Tolson, R. F.; Harvey, N.; Lodge, S. L.; Chetwynd, A. J.; Cannet, C.; Fang, F.; Pearce, J. T. M.; Lewis, M. R.; Viant, M. R.; Lindon, J. C.; Spraul, M.; Schafer, H.; Nicholson, J. K. *Anal. Chem.* **2018**, *90*, 11962−11971.
(12) Mallol, R.; Amigó, N.; Rodríguez, M. A.; Heras, M.; Vinaixa, M.; Plana, N.; Rock, E.; Ribalta, J.; Yanes, O.; Masana, L.; Correig, X. *J. Lipid Res.* **2015**, *56*, 737−746.
(13) Bell, J. D.; Brown, J. C.; Sadler, P. J. *NMR Biomed.* **1989**, *2*, 246−256.
(14) Mehta, N. N.; Dey, A. K.; Maddineni, R.; Kraus, W. E.; Huffman, K. M. *Am. J. Prev. Cardiol.* **2020**, *4*, No. 100120.
(15) Dudka, I.; Chachaj, A.; Sebastian, A.; Tański, W.; Stenlund, H.; Gröbner, G.; Szuba, A. *J. Pharm. Biomed. Anal.* **2021**, *197*, No. 113971.
(16) Prokic, I.; Lahousse, L.; de Vries, M.; Liu, J.; Kalaoja, M.; Vonk, J. M.; van der Plaat, D. A.; van Diemen, C. C.; van der Spek, A.; Zhernakova, A.; Fu, J.; Ghanbari, M.; Ala-Korpela, M.; Kettunen, J.; Havulinna, A. S.; Perola, M.; Salomaa, V.; Lind, L.; Arnlov, J.; Stricker, B. H. C.; Brusselle, G. G.; Boezen, H. M.; van Duijn, C. M.; Amin, N. *BMC Pulm. Med.* **2020**, *20*, 193.
(17) Buszko, M.; Nita-Lazar, A.; Park, J.-H.; Schwartzberg, P. L.; Verthelyi, D.; Young, H. A.; Rosenberg, A. S. *Nat. Immunol.* **2021**, *22*, 404−411.
(18) Medzhitov, R. *Nature* **2008**, *454*, 428−435.
(19) Kany, S.; Vollrath, J. T.; Relja, B. *Int. J. Mol. Sci.* **2019**, *20*, 6008.
(20) Gullestad, L.; Ueland, T.; Vinge, L. E.; Finsen, A.; Yndestad, A.; Aukrust, P. *Cardiology* **2012**, *122*, 23−35.
(21) Srikakulapu, P.; McNamara, C. A. *Arterioscler., Thromb., Vasc. Biol.* **2020**, *40*, 1110−1122.
(22) Sproston, N. R.; Ashworth, J. J. *Front. Immunol.* **2018**, *9*, 754.
(23) Ricciotti, E.; FitzGerald, G. A. *Arterioscler., Thromb., Vasc. Biol.* **2011**, *31*, 986−1000.
(24) Otvos, J. D.; Shalaurova, I.; Wolak-Dinsmore, J.; Connelly, M. A.; Mackey, R. H.; Stein, J. H.; Tracy, R. P. *Clin. Chem.* **2015**, *61*, 714−723.
(25) Bell, J. D.; Brown, J. C. C.; Nicholson, J. K.; Sadler, P. J. *FEBS Lett.* **1987**, *215*, 311−315.
(26) Ritchie, S. C.; Wurtz, P.; Nath, A. P.; Abraham, G.; Havulinna, A. S.; Fearnley, L. G.; Sarin, A. P.; Kangas, A. J.; Soininen, P.; Aalto, K.; Seppala, I.; Raitoharju, E.; Salmi, M.; Maksimow, M.; Mannisto, S.; Kahonen, M.; Juonala, M.; Ripatti, S.; Lehtimaki, T.; Jalkanen, S.; Perola, M.; Raitakari, O.; Salomaa, V.; Ala-Korpela, M.; Kettunen, J.; Inouye, M. *Cell Syst.* **2015**, *1*, 293−301.
(27) Holmes, E.; Wist, J.; Masuda, R.; Lodge, S.; Nitschke, P.; Kimhofer, T.; Loo, R. L.; Begum, S.; Boughton, B.; Yang, R.;

Morillon, A.-C.; Chin, S.-T.; Hall, D.; Ryan, M.; Bong, S.-H.; Gay, M.; Edgar, D. W.; Lindon, J. C.; Richards, T.; Yeap, B. B.; Pettersson, S.; Spraul, M.; Schaefer, H.; Lawler, N. G.; Gray, N.; Whiley, L.; Nicholson, J. K. *J. Proteome Res.* **2021**, *20*, 3315−3329.
(28) Dierckx, T.; Verstockt, B.; Vermeire, S.; van Weyenbergh, J. *J. Crohns. Colitis* **2019**, *13*, 389−394.
(29) Fuertes-Martín, R.; Taverner, D.; Vallvé, J.-C.; Paredes, S.; Masana, L.; Correig Blanchar, X.; Amigó Grau, N. *J. Proteome Res.* **2018**, *17*, 3730−3739.
(30) Dierckx, T.; Chiche, L.; Daniel, L.; Lauwerys, B.; Van Weyenbergh, J.; Jourde-Chiche, N. *J. Clin. Med. Res.* **2020**, *9*, 970.
(31) Joshi, A. A.; Lerman, J. B.; Aberra, T. M.; Afshar, M.; Teague, H. L.; Rodante, J. A.; Krishnamoorthy, P.; Ng, Q.; Aridi, T. Z.; Salahuddin, T.; Natarajan, B.; Lockshin, B. N.; Ahlman, M. A.; Chen, M. Y.; Rader, D. J.; Reilly, M. P.; Remaley, A. T.; Bluemke, D. A.; Playford, M. P.; Gelfand, J. M.; Mehta, N. N. *Circ. Res.* **2016**, *119*, 1242−1253.
(32) Gruppen, E. G.; Connelly, M. A.; Sluiter, W. J.; Bakker, S. J. L.; Dullaart, R. P. F. *Clin. Chim. Acta* **2019**, *488*, 7−12.
(33) Jang, S.; Ogunmoroti, O.; Ndumele, C. E.; Zhao, D.; Rao, V. N.; Fashanu, O. E.; Tibuakuu, M.; Otvos, J. D.; Benson, E. M.; Ouyang, P.; Michos, E. D. *Circ. Heart Fail.* **2020**, *13*, No. e007067.
(34) Titan, S. M.; Pecoits-Filho, R.; Barreto, S. M.; Lopes, A. A.; Bensenor, I. J.; Lotufo, P. A. *BMC Nephrol.* **2017**, *18*, 367.
(35) Lodge, S.; Nitschke, P.; Kimhofer, T.; Wist, J.; Bong, S.-H.; Loo, R. L.; Masuda, R.; Begum, S.; Richards, T.; Lindon, J. C.; Bermel, W.; Reinsperger, T.; Schaefer, H.; Spraul, M.; Holmes, E.; Nicholson, J. K. *Anal. Chem.* **2021**, *93*, 3976−3986.
(36) Fan, J.; Wang, H.; Ye, G.; Cao, X.; Xu, X.; Tan, W.; Zhang, Y. *Metabolism* **2020**, *107*, No. 154243.
(37) Masana, L.; Correig, E.; Ibarretxe, D.; Anoro, E.; Arroyo, J. A.; Jericó, C.; Guerrero, C.; la Miret, M.; Näf, S.; Pardo, A.; Perea, V.; Pérez-Bernalte, R.; Plana, N.; Ramírez-Montesinos, R.; Royuela, M.; Soler, C.; Urquizu-Padilla, M.; Zamora, A.; Pedro-Botet, J. *Sci. Rep.* **2021**, *11*, 7217.
(38) Wei, X.; Zeng, W.; Su, J.; Wan, H.; Yu, X.; Cao, X.; Tan, W.; Wang, H. *J. Clin. Lipidol.* **2020**, *14*, 297−304.
(39) Tanaka, S.; De Tymowski, C.; Assadi, M.; Zappella, N.; Jean-Baptiste, S.; Robert, T.; Peoc'h, K.; Lortat-Jacob, B.; Fontaine, L.; Bouzid, D.; Tran-Dinh, A.; Tashk, P.; Meilhac, O.; Montravers, P. *PLoS One* **2020**, *15*, No. e0239573.
(40) Gray, N.; Lawler, N. G.; Zeng, A. X.; Ryan, M.; Bong, S. H.; Boughton, B. A.; Bizkarguenaga, M.; Bruzzone, C.; Embade, N.; Wist, J.; Holmes, E.; Millet, O.; Nicholson, J. K.; Whiley, L. *Metabolites* **2021**, *11*, 467.
(41) Chen, Y.-M.; Zheng, Y.; Yu, Y.; Wang, Y.; Huang, Q.; Qian, F.; Sun, L.; Song, Z.-G.; Chen, Z.; Feng, J.; An, Y.; Yang, J.; Su, Z.; Sun, S.; Dai, F.; Chen, Q.; Lu, Q.; Li, P.; Ling, Y.; Yang, Z.; Tang, H.; Shi, L.; Jin, L.; Holmes, E. C.; Ding, C.; Zhu, T.-Y.; Zhang, Y.-Z. *EMBO J.* **2020**, *39*, No. e105896.
(42) Barberis, E.; Timo, S.; Amede, E.; Vanella, V. V.; Puricelli, C.; Cappellano, G.; Raineri, D.; Cittone, M. G.; Rizzi, E.; Pedrinelli, A. R.; Vassia, V.; Casciaro, F. G.; Priora, S.; Nerici, I.; Galbiati, A.; Hayden, E.; Falasca, M.; Vaschetto, R.; Sainaghi, P. P.; Dianzani, U.; Rolla, R.; Chiocchetti, A.; Baldanzi, G.; Marengo, E.; Manfredi, M. *Int. J. Mol. Sci.* **2020**, *21*, No. 228623.
(43) Queiroz, A.; Pinto, I. F. D.; Lima, M.; Giovanetti, M.; de Jesus, J. G.; Xavier, J.; Barreto, F. K.; Canuto, G. A. B.; do Amaral, H. R.; de Filippis, A. M. B.; Mascarenhas, D. L.; Falcão, M. B.; Santos, N. P.; de Azevedo, V. A. C.; Yoshinaga, M. Y.; Miyamoto, S.; Alcantara, L. C. J. *Front. Microbiol.* **2019**, *10*, 753.
(44) Bai, Y.; Huang, W.; Li, Y.; Lai, C.; Huang, S.; Wang, G.; He, Y.; Hu, L.; Chen, C. *Biosci. Rep.* **2021**, *41*, No. BSR20204305.
(45) Wu, Q.; Zhou, L.; Sun, X.; Yan, Z.; Hu, C.; Wu, J.; Xu, L.; Li, X.; Liu, H.; Yin, P.; Li, K.; Zhao, J.; Li, Y.; Wang, X.; Li, Y.; Zhang, Q.; Xu, G.; Chen, H. *Sci. Rep.* **2017**, *7*, 9110.
(46) Carr, H. Y.; Purcell, E. M. *Phys. Rev.* **1954**, *94*, 630−638.
(47) Meiboom, S.; Gill, D. *Rev. Sci. Instrum.* **1958**, *29*, 688−691.
(48) Ala-Korpela, M.; Lankinen, N.; Salminen, A.; Suna, T.; Soininen, P.; Laatikainen, R.; Ingman, P.; Jauhiainen, M.; Taskinen, M.-R.; Héberger, K.; Kaski, K. *Atherosclerosis* **2007**, *190*, 352−358.
(49) Fuertes-Martín, R.; Correig, X.; Vallvé, J.-C.; Amigó, N. *J. Clin. Med. Res.* **2020**, *9*, 354.
(50) Liu, M.; Nicholson, J. K.; Lindon, J. C. *Anal. Chem.* **1996**, *68*, 3370−3376.
(51) Martin-Pastor, M. *J. Agric. Food Chem.* **2014**, *62*, 1190−1197.
(52) Masuda, R.; Lodge, S.; Nitschke, P.; Spraul, M.; Schaefer, H.; Bong, S.-H.; Kimhofer, T.; Hall, D.; Loo, R. L.; Bizkarguenaga, M.; Bruzzone, C.; Gil-Redondo, R.; Embade, N.; Mato, J. M.; Holmes, E.; Wist, J.; Millet, O.; Nicholson, J. K. *J. Proteome Res.* **2021**, *20*, 4139−4152.
(53) Bruzzone, C.; Bizkarguenaga, M.; Gil-Redondo, R.; Diercks, T.; Arana, E.; García de Vicuña, A.; Seco, M.; Bosch, A.; Palazón, A.; San Juan, I.; Laín, A.; Gil-Martínez, J.; Bernardo-Seisdedos, G.; Fernández-Ramos, D.; Lopitz-Otsoa, F.; Embade, N.; Lu, S.; Mato, J. M.; Millet, O. *iScience* **2020**, *23*, No. 101645.
(54) Dona, A. C.; Jimenez, B.; Schafer, H.; Humpfer, E.; Spraul, M.; Lewis, M. R.; Pearce, J. T.; Holmes, E.; Lindon, J. C.; Nicholson, J. K. *Anal. Chem.* **2014**, *86*, 9887−9894.
(55) Akoka, S.; Barantin, L.; Trierweiler, M. *Anal. Chem.* **1999**, *71*, 2554−2557.
(56) Kimhofer, T.; Lodge, S.; Whiley, L.; Gray, N.; Loo, R. L.; Lawler, N. G.; Nitschke, P.; Bong, S. H.; Morrison, D. L.; Begum, S.; Richards, T.; Yeap, B. B.; Smith, C.; Smith, K. C. G.; Holmes, E.; Nicholson, J. K. *J. Proteome Res.* **2020**, 4442.
(57) Wang, Q.; Würtz, P.; Auro, K.; Mäkinen, V.-P.; Kangas, A. J.; Soininen, P.; Tiainen, M.; Tynkkynen, T.; Jokelainen, J.; Santalahti, K.; Salmi, M.; Blankenberg, S.; Zeller, T.; Viikari, J.; Kähönen, M.; Lehtimäki, T.; Salomaa, V.; Perola, M.; Jalkanen, S.; Järvelin, M.-R.; Raitakari, O. T.; Kettunen, J.; Lawlor, D. A.; Ala-Korpela, M. *BMC Med.* **2016**, *14*, 205.
(58) Rauschert, S.; Gázquez, A.; Uhl, O.; Kirchberg, F. F.; Demmelmair, H.; Ruíz-Palacios, M.; Prieto-Sánchez, M. T.; Blanco-Carnero, J. E.; Nieto, A.; Larqué, E.; Koletzko, B. *Lipids Health Dis.* **2019**, *18*, 20.
(59) Lodge, S.; Nitschke, P.; Kimhofer, T.; Coudert, J. D.; Begum, S.; Bong, S.-H.; Richards, T.; Edgar, D.; Raby, E.; Spraul, M.; Schaefer, H.; Lindon, J. C.; Loo, R. L.; Holmes, E.; Nicholson, J. K. *J. Proteome Res.* **2021**, *20*, 1382−1396.
(60) Nicholson, J. K. *Phenomics* **2021**, 143.

https://doi.org/10.1021/acs.analchem.1c04576
Anal. Chem. XXXX, XXX, XXX−XXX